Available online at www.sciencedirect.com
SCIENCE DIRECT®
International Journal of Heat and Mass Transfer 48 (2005) 3660–3673
International Journal of HEAT and MASS TRANSFER
www.elsevier.com/locate/ijhmt

Correlating equations for free convection heat transfer from horizontal isothermal cylinders set in a vertical array

Massimo Corcione *

Dipartimento di Fisica Tecnica, University of Rome "La Sapienza", via Eudossiana 18, Rome 00184, Italy

Received 17 May 2004
Available online 24 May 2005

Abstract

Steady laminar free convection from flat vertical arrays of equally-spaced, horizontal isothermal cylinders set in free air, is studied numerically. A specifically developed computer-code based on the SIMPLE-C algorithm is used for the solution of the mass, momentum and energy transfer governing equations. Simulations are performed for arrays of 2–6 circular cylinders, for center-to-center separation distances from 2 up to more than 50 cylinder-diameters, and for values of the Rayleigh number based on the cylinder-diameter in the range between 5×10^2 and 5×10^5. It is found that the heat transfer rate at the bottom cylinder remains the same as a single cylinder. In contrast, the downstream cylinders may exhibit either enhanced or reduced Nusselt numbers depending on their location in the array and on the geometry of the array. Heat transfer dimensionless correlating equations are proposed both for any individual cylinder in the array and for the whole tube-array. New correlation-equations for the calculation of the heat transfer rate from a single cylinder to the surrounding air are also proposed and compared to those available in the open literature.

Keywords: Free convection; Horizontal cylinders; Vertical array; Correlating equations; Numerical analysis

1. Introduction

Free convection heat transfer from arrays of horizontal cylinders set in free space has a practical relevance to many engineering applications, e.g., space heating, heating of high-viscosity oils for pumping ease, heating or cooling of fluids in process plants, operation and safety of nuclear reactors, as well as cooling of electronic devices and refrigeration condensers.

The investigations conducted on this subject are relatively few and mainly based on an experimental approach, chiefly due to the larger theoretical complexities involved in comparison with the equivalent forced convection case, where (a) the mass flow rate is known, (b) the momentum and energy equations are uncoupled, provided that the physical properties of the fluid are assumed to be constant, and (c) the governing equations may be solved for a single representative element of the array, provided that the fluid flow is assumed to be fully developed.

The first documented work in this field was made by Eckert and Soehngen [1] who carried out demonstrative experiments with three horizontal isothermal cylinders of 22.3-mm dia arranged one above the other, both in-line and staggered, for Grashof numbers based on the cylinder-diameter equal to 34,300 and 14,650,

* Tel.: +39 06 44 58 54 43; fax: +39 06 48 80 120.
E-mail address: massimo.corcione@uniroma1.it

0017-9310/$ - see front matter © 2005 Elsevier Ltd. All rights reserved.
doi:10.1016/j.ijheatmasstransfer.2005.01.010

Nomenclature

D	diameter of the cylinders
$\mathbf{g}$	gravity vector
g	gravitational acceleration
H	overall height of the array
k	thermal conductivity of the fluid
N	number of cylinders in the array
N_i	ordinal number of the ith cylinder in the array
Nu_a	average Nusselt number of the whole tube-array
Nu_i	average Nusselt number of the ith cylinder in the array
Nu_0	average Nusselt number of the single cylinder
$Nu_i(\theta)$	local Nusselt number of the ith cylinder in the array
p	dimensionless pressure
Pr	Prandtl number = ν/α
Q	heat transfer rate
q	heat flux
r	dimensionless radial coordinate
Ra	Rayleigh number based on the cylinder-diameter = $g\beta(t_w - t_\infty)D^3/\alpha\nu$
Ra_H	Rayleigh number based on the overall height of the array = $g\beta(t_w - t_\infty)H^3/\alpha\nu$
S	center-to-center separation distance
T	dimensionless temperature
t	temperature
U	dimensionless vertical or radial velocity component
U^*	dimensionless radial velocity = $U \times Pr \times Ra^{-0.25}$
$\mathbf{V}$	dimensionless velocity vector
V	dimensionless horizontal or tangential velocity component
V^*	dimensionless tangential velocity = $V \times Pr \times Ra^{-0.25}$
X	dimensionless vertical coordinate
x	center-to-center distance of the ith cylinder from the bottom cylinder
Y	dimensionless horizontal coordinate
Y^*	dimensionless radial distance from the cylinder surface = $(r - 0.5) \times Ra^{-0.25}$

Greek symbols

α	thermal diffusivity of the fluid
β	coefficient of volumetric thermal expansion of the fluid
ν	kinematic viscosity of the fluid
θ	dimensionless polar coordinate
ρ	density of the fluid

Subscripts

cr	critical value
w	referred to the cylinder surface
max	maximum value
∞	referred to the undisturbed fluid

respectively. When the cylinders were set in a vertical array, they found that the heat transfer rate at the bottom cylinder remained the same as a single cylinder, whilst that at the other cylinders decreased with elevation in the array. Once the cylinders were arranged in a staggered array, the Nusselt number of the bottom cylinder remained unchanged, but that of the offset middle cylinder displayed a slight enhancement with respect to the single cylinder.

Experimental investigations have been performed under conditions of uniform heat flux by Lieberman and Gebhart [2], who used a flat array of 10 wires of 0.127-mm dia with six spacings from 37.5 to 225 diameters and four orientation angles from 0° to 90°, for a Grashof number 1.75×10^{-2}, and by Marsters [3], who used a vertical array of three, five and nine cylinders of 6.35-mm dia with five spacings from 2 to 20 diameters, for Grashof numbers in the range between 750 and 2000. In both studies, it was again found that the Nusselt number of the bottom cylinder was substantially identical to that for a single cylinder, even for the closest center-to-center separation distance investigated. In contrast, the upper cylinders exhibited reduced Nusselt numbers at close spacings and enhanced Nusselt numbers at large spacings.

Same type of results were obtained by Sparrow and Niethammer [4], who carried out an experimental study on a vertical array of two isothermal cylinders of 37.9-mm dia with different spacings from 2 to 9 diameters, for Rayleigh numbers in the range between 2×10^4 and 2×10^5. In their work, the authors evaluated also the influence of the cylinder-to-cylinder temperature imbalance, by varying the wall-to-ambient temperature difference for the lower cylinder between zero and three times that for the upper cylinder, showing that its effects are of major importance at small spacings, being practically negligible at large spacings.

The influence of the separation distance on the enhancement or degradation of the heat transfer rate at the downstream cylinders found in the aforementioned

studies, is a strict consequence of the two opposite effects which originate from the warm plume spawned by the preceding cylinder. In fact, the hot buoyant flow from the upstream cylinder acts as a forced convection field wherein the downstream cylinder is embedded. On the other side, the upward-moving warm plume causes a decrease in the temperature difference between the surface of the downstream cylinder and the adjacent fluid. The first effect, which tends to increase the heat transfer rate at the downstream cylinder, prevails at large spacings. The second effect, which tends to decrease the heat transfer rate at the downstream cylinder, is of major importance at close spacings. This may be explained through the theoretical results obtained by Gebhart et al. for a plume above a horizontal line source [5]. In fact, they demonstrated that the centerline temperature of the plume decreases as the inverse of the three-fifths power of the distance above the source, whilst the centerline velocity of the plume increases as the fifth power of the distance above the source. Hence, from a critical distance onwards, the velocity effect must outweigh the effect of the increased fluid temperature, thus bringing to the cited enhancement of the Nusselt number of the downstream cylinder.

On the other hand, it seems reasonable to assume that as the distance above the source increases further, also the velocity effect must progressively reduce up to vanishing. Thus, the behavior of the downstream cylinder at very large spacings is expected to resemble that typical for a single cylinder, which implies the existence of an optimum separation distance at which the amount of heat transferred is maximum. Indeed, this was observed by Lieberman and Gebhart [2], whose experimental data indicate the occurrence of a very shallow maximum of the average Nusselt number of the array at a separation distance around 120 wire-diameters. Also Sparrow and Niethammer [4] suggested the presence of a maximum at a separation distance around 8 tube-diameters, although upon the basis of a very short number of experimental data.

Other successive experimental studies on free convection heat transfer from arrays of horizontal isothermal cylinders brought substantially to same kind of results. Among them, leaving aside all the papers which do not deal strictly with vertical geometries (see, e.g., [6,7]), it seems worth mentioning the studies performed by Tokura et al. [8], who used vertical arrays of two, three and five cylinders of 22.2-mm, 28.5-mm and 38-mm dia with spacings up to 20 diameters, for Grashof numbers in the range between 4×10^4 and 4×10^5, and by Sadegh Sadeghipour and Asheghi [9], who used a vertical array of two to eight 6.6-mm dia cylinders with spacings from 3.5 to 30.5 diameters, for Rayleigh numbers 500, 600, and 700. In both papers an empirical correlation to predict the average Nusselt number of the whole array in the experimented range of the Rayleigh number is proposed. In addition, a shallow maximum for the heat transfer rate is reported for a spacing of nearly 15 cylinder-diameters, although, in some cases, the maximum is difficult to detect, being concealed by the spreading of the experimental data. In this connection, it seems interesting to note that the location of the maximum reported by Tokura et al. [8] is rather different from that indicated by Sparrow and Niethammer [4], despite both studies were conducted practically under same conditions, using cylinders of the same diameter.

As far as the numerical studies available in the literature are concerned, Farouk and Guceri [10] carried out a study of laminar and turbulent free convection from single and double, both in-line and staggered, horizontal rows of closely spaced isothermal cylinders, showing that the heat transfer rates were strongly dependent on both the vertical and the horizontal spacings. More recently, Chouikh et al. [11] conducted a numerical study of laminar free convection from an isothermal two-cylinder vertical array with spacings in the range between 2 and 6 diameters, for Rayleigh numbers in the range between 10^2 and 10^4, with results consistent with those of the earlier experimental studies.

According to what has been discussed above, the main phenomenologic aspects of the problem are well understood, but, on the other hand, a short availability of data and, above all, an almost complete lack of correlations for predicting the thermal behavior of individual cylinders set in a vertical array, as well as that of the whole array, comes out (actually, the correlations proposed for the whole array by Tokura et al. [8] and by Sadegh Sadeghipour and Asheghi [9] are referred to ranges of the Rayleigh number which seem too narrow for extensive practical uses).

In this framework, the aim of the present paper is to carry out a numerical analysis of free convection from flat vertical arrays of equally-spaced, horizontal isothermal cylinders, so as to derive heat transfer dimensionless correlating equations for any individual cylinder in the array and for the whole tube-array, spanning across a range of the Rayleigh number definitely wider than those of other empirical equations available in the open literature. The study is performed under the assumption of steady laminar flow, for arrays of 2–6 circular cylinders, for center-to-center separation distances from 2 up to more than 50 cylinder-diameters, and for values of the Rayleigh number based on the cylinder-diameter in the range between 5×10^2 and 5×10^5.

2. Mathematical formulation

The flat vertical array of equally-spaced, horizontal circular cylinders depicted in Fig. 1 is considered. The diameter D of the cylinders, their number N, and their

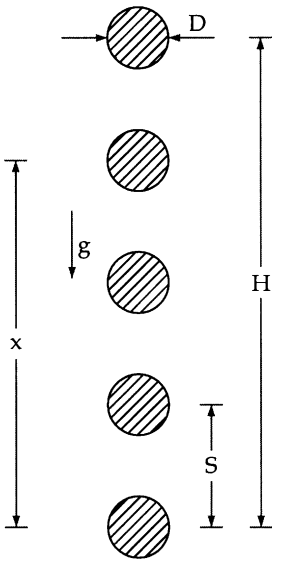

Fig. 1. Sketch of the tube-array.

separation distance S are assigned. The height of the array, i.e., the center-to-center separation distance between the bottom and top cylinders, is then $H = S \times (N - 1)$. Free convection heat transfer occurs between the cylinder surfaces, kept at uniform temperature t_w and the surrounding undisturbed fluid reservoir, assumed at uniform temperature t_∞.

The buoyancy-induced flow is considered to be steady, two-dimensional, and laminar. The fluid is assumed to be incompressible, with constant physical properties and negligible viscous dissipation and pressure work. The buoyancy effects on momentum transfer are taken into account through the Boussinesq approximation.

Once the above assumptions are employed in the conservation equations of mass, momentum, and energy, the following set of dimensionless governing equations is obtained:

$$\nabla \cdot \mathbf{V} = 0 \tag{1}$$

$$(\mathbf{V} \cdot \nabla)\mathbf{V} = -\nabla p + \nabla^2 \mathbf{V} - \frac{Ra}{Pr} T \frac{\mathbf{g}}{g} \tag{2}$$

$$(\mathbf{V} \cdot \nabla) T = \frac{1}{Pr} \nabla^2 T \tag{3}$$

where $\mathbf{V}$ is the velocity vector having dimensionless velocity components U and V normalized with ν/D; T is the dimensionless temperature excess over the uniform temperature of the surrounding undisturbed fluid normalized with the temperature difference $(t_w - t_\infty)$; p is the dimensionless pressure normalized with $\rho_\infty \nu^2/D^2$; $\mathbf{g}$ is the gravity vector; $Ra = g\beta(t_w - t_\infty)D^3/\nu\alpha$ is the Rayleigh number based on the cylinder-diameter; and $Pr = \nu/\alpha$ is the Prandtl number.

The related boundary conditions are $T = 1$ and $\mathbf{V} = 0$ at the cylinder surfaces, and $T = 0$ and $\mathbf{V} = 0$ at very large distance from the tube-array.

3. Discretization grid system

The finite-difference solution of the governing equations (1)–(3) with the proper boundary conditions requires that a discretization grid system is established across the whole integration domain.

In this connection, a Cartesian grid could in principle be adopted. However, once the node-spacing were adjusted so that the near-wall nodes fell exactly on the cylinder surfaces, the resulting discretization grid would be characterized by a low density of nodes precisely where an accurate numerical solution demands a fine spacing, i.e., in the region of the front and rear stagnation points of each cylinder.

For this reason the problem is solved by the employment of a cylindrical polar grid in the proximity of each cylinder, and of a Cartesian grid across the remainder of the integration domain. Furthermore, a condition of symmetry about the vertical midplane of the array is assumed, thus obtaining the halving of the size of the integration domain. The integration domain is therefore assumed to extend from the vertical symmetry midplane up to a rectangular boundary set sufficiently far away from the array to represent the so-called outer boundary, as sketched in the left panel of Fig. 2, where the coordinate systems adopted are also represented. In particular, the r and θ coordinates of the polar systems are measured from the center of the cylinders, and anticlockwise from downwards, respectively. In the polar systems, U is the radial velocity component, and V is the tangential velocity component. As concerns the Cartesian system, whose origin is taken at the center of the bottom cylinder, the X-axis is vertical and pointing upwards in the direction opposite to the gravity vector, whilst the Y-axis is horizontal. In this system, U is the vertical velocity component, and V is the horizontal velocity component.

According to the discretization scheme originally developed by Launder and Massey [12], the cylindrical polar grids and the Cartesian grid, which are entirely independent of one another, overlap with no attempt of node-matching. Their connection is provided by a row of false nodes, one for each neighboring grid, located beyond their intersection, as depicted in the middle panel of Fig. 2.

4. Boundary conditions

The boundary conditions required for the numerical solution of the governing equations (1)–(3) have to be

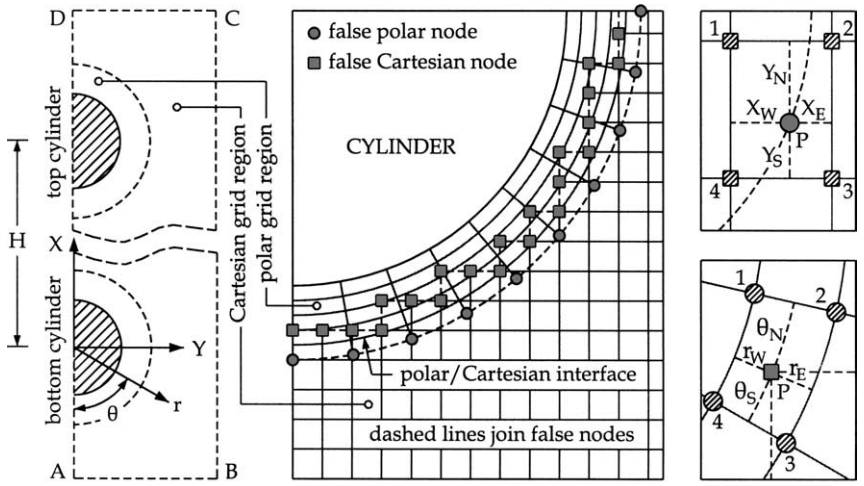

Fig. 2. Sketch of the coordinate systems and of the discretization-grid system.

specified at each of the boundary lines which enclose the two-dimensional integration domain assumed for the present study. As specifically concerns the artificially imposed outer boundary, once this is placed sufficiently far away from the tube-array, the fluid may reasonably be assumed to enter or leave the integration flow-domain in the direction normal to the boundary. The entering fluid is assumed at the ambient temperature. As concerns the leaving fluid, whose temperature is not known a priori, a zero temperature gradient normal to the pseudo-boundary is assumed, thus implying that the local heat transfer is dominated by convection rather than by conduction, provided that the outflow velocity is sufficiently large.

The following boundary conditions are applied:

(a) at the left symmetry line A–D

$$\frac{\partial U}{\partial Y}=0 \quad V=0 \quad \frac{\partial T}{\partial Y}=0 \tag{4}$$

(b) on the cylinder surfaces

$$U=0 \quad V=0 \quad T=1 \tag{5}$$

(c) at the bottom boundary line A–B

$$\frac{\partial U}{\partial X}=0 \quad V=0$$
$$T=0 \text{ if } U\geqslant 0 \quad \text{or} \quad \frac{\partial T}{\partial X}=0 \text{ if } U<0 \tag{6}$$

(d) at the right boundary line B–C

$$U=0 \quad \frac{\partial V}{\partial Y}=0$$
$$T=0 \text{ if } V<0 \quad \text{or} \quad \frac{\partial T}{\partial Y}=0 \text{ if } V\geqslant 0 \tag{7}$$

(e) at the top boundary line C–D

$$\frac{\partial U}{\partial X}=0 \quad V=0$$
$$T=0 \text{ if } U<0 \quad \text{or} \quad \frac{\partial T}{\partial X}=0 \text{ if } U\geqslant 0 \tag{8}$$

Moreover, as far as the intersections between polar and Cartesian grids are concerned, the values of the dependent variables at the false nodes are obtained by a linear interpolation of the values at the four surrounding nodes. With reference to the notations indicated in the right panels of Fig. 2, the value of the general variable ϕ at any false Cartesian or polar node is calculated through the following equations, respectively:

$$\phi_P=\frac{\phi_1 X_E Y_S+\phi_2 X_W Y_S+\phi_3 X_W Y_N+\phi_4 X_E Y_N}{(X_W+X_E)(Y_S+Y_N)} \tag{9}$$

$$\phi_P=\frac{\phi_1 r_E \theta_S+\phi_2 r_W \theta_S+\phi_3 r_W \theta_N+\phi_4 r_E \theta_N}{(r_W+r_E)(\theta_S+\theta_N)} \tag{10}$$

5. Solution procedure

The set of governing equations (1)–(3) with the boundary conditions (4)–(10) is solved through a control-volume formulation of the finite-difference method. The pressure–velocity coupling is handled by the SIMPLE-C algorithm by Van Doormaal and Raithby [13], which is essentially a more implicit variant of the SIMPLE algorithm by Patankar and Spalding [14]. The convective fluxes across the surfaces of the control volumes are evaluated by the QUICK discretization scheme by Leonard [15]. Details on the SIMPLE procedure may be found in Patankar [16]. Studies on the comparative performance of different discretization schemes for the

evaluation of the interface convective fluxes, as well as studies on enhanced variants of the SIMPLE algorithm, are widely available and well referenced in the open literature (see, e.g., [17]).

Fine uniform mesh-spacings are used for the discretization of both the polar grid regions and the Cartesian grid region. Starting from specified first-approximation distributions of the dependent variables across the integration domain, the discretized governing equations are solved iteratively through a line-by-line application of the Thomas algorithm. Under-relaxation is used to ensure the convergence of the iterative procedure. The solution is considered to be fully converged when the maximum absolute values of both the mass source and the percent changes of the dependent variables at any grid-node from iteration to iteration are smaller than prescribed values, i.e., 10^{-4} and 10^{-6}, respectively.

After convergence is attained, the local and average Nusselt numbers $Nu_i(\theta)$ and Nu_i of any ith cylinder in the array are calculated:

$$Nu_i(\theta) = \frac{qD}{k(t_w - t_\infty)} = -\left.\frac{\partial T}{\partial r}\right|_{r=0.5} \tag{11}$$

$$Nu_i = \frac{Q}{\pi k(t_w - t_\infty)} = -\frac{1}{\pi}\int_0^\pi \left.\frac{\partial T}{\partial r}\right|_{r=0.5} d\theta \tag{12}$$

where q is the heat flux and Q is the heat transfer rate. The temperature gradients at the cylinder surfaces are evaluated by assuming a second-order temperature profile among each wall-node and the next two fluid-nodes. The integrals are approximated by the trapezoid rule. The average Nusselt number of the whole array Nu_a is then obtained as the arithmetic mean value of the average Nusselt numbers Nu_i of the individual cylinders in the array:

$$Nu_a = \frac{1}{N}\sum_{i=1}^{N} Nu_i \tag{13}$$

Tests on the dependence of the results obtained on the mesh-spacing of both the polar and the Cartesian discretization grids, as well as on the thickness of the polar grid regions, and on the extension of the whole computational domain, have been performed for a wide variety of geometrical configurations analyzed and of Rayleigh numbers investigated. In particular, the optimal grid-size values, and the optimal positions of the polar/Cartesian interface and of the outer pseudo-boundary, i.e., those used for computations, which represent a good compromise between solution accuracy and computational time required, are assumed as those over which further refinements or further displacements do not produce noticeable modifications in both the heat transfer rates and the predicted flow field. Namely when, for each cylinder in the array, the percent changes of the local and average Nusselt numbers $Nu_i(\theta)$ and Nu_i defined above, as well as the percent change of the maximum value of the tangential velocity component at $\theta = 90°$ are smaller than prescribed accuracy values, i.e., 1% and 2%, respectively. Typically: (a) the number of nodal points ($r \times \theta$) of the polar discretization grids lie in the range between 45×72 and 135×90, (b) the thickness of the polar grid regions varies between one and five times the cylinder-diameter, and (c) the extent of the whole integration flow-domain ranges between two and twenty times the cylinder-diameter, depending on the Rayleigh number, as well as on the number of cylinders in the array, and on their center-to-center separation distance.

Furthermore, in order to validate the numerical code and the composite-grid discretization scheme specifically

Table 1
Comparison of the present solutions with the bench mark solutions of Saitoh et al. and with the results of Wang et al. and Kuehn and Goldstein

Ra		*Nu*(θ)							*Nu*
		θ = 0°	30°	60°	90°	120°	150°	180°	
10^3	Present	3.789	3.755	3.640	3.376	2.841	1.958	1.210	3.013
	Saitoh et al. [18]	3.813	3.772	3.640	3.374	2.866	1.975	1.218	3.024
	Wang et al. [19]	3.860	3.820	3.700	3.450	2.930	1.980	1.200	3.060
	Kuehn and Goldstein [20]	3.890	3.850	3.720	3.450	2.930	2.010	1.220	3.090
10^4	Present	5.986	5.931	5.756	5.406	4.716	3.293	1.532	4.819
	Saitoh et al. [18]	5.995	5.935	5.750	5.410	4.764	3.308	1.534	4.826
	Wang et al. [19]	6.030	5.980	5.800	5.560	4.870	3.320	1.500	4.860
	Kuehn and Goldstein [20]	6.240	6.190	6.010	5.640	4.820	3.140	1.460	4.940
10^5	Present	9.694	9.595	9.297	8.749	7.871	5.848	1.989	7.886
	Saitoh et al. [18]	9.675	9.577	9.278	8.765	7.946	5.891	1.987	7.898
	Wang et al. [19]	9.800	9.690	9.480	8.900	8.000	5.800	1.940	7.970
	Kuehn and Goldstein [20]	10.150	10.030	9.650	9.020	7.910	5.290	1.720	8.000

developed for the present study, the local and average Nusselt numbers obtained for a single cylinder at Rayleigh numbers 10^3, 10^4, and 10^5, have been compared with the benchmark data by Saitoh et al. [18], as shown in Table 1, where the numerical results of Wang et al. [19] and of Kuehn and Goldstein [20] are also reported. In particular, it may be seen that the local results are well within ±1% of the benchmark data, whilst the absolute value of the largest percent difference between the average Nusselt numbers is 0.36%. The computed distributions of the dimensionless temperature T, and of the dimensionless radial and tangential velocities $U^* = U \times Pr \times Ra^{-0.25}$ and $V^* = V \times Pr \times Ra^{-0.25}$ versus the dimensionless radial distance from the cylinder surface $Y^* = (r - 0.5) \times Ra^{-0.25}$ at the Rayleigh number 10^5 are then compared (a) with the experimental data of Kuehn and Goldstein [20], (b) with the numerical results of Saitoh et al. [18], Wang et al. [19], and Kuehn and Goldstein [20], and (c) with the analytical results of Chiang and Kaye [21], as reported in Figs. 3, 4, and 5, respectively.

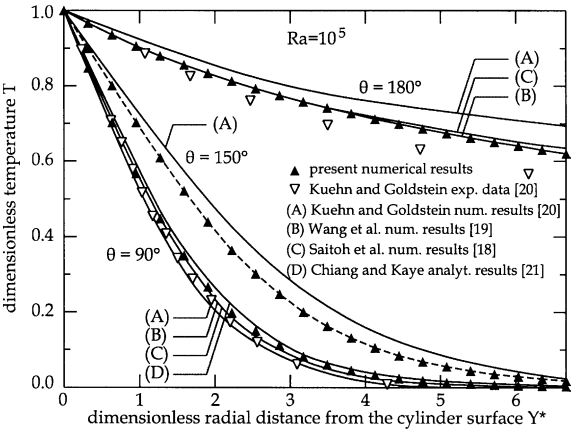

Fig. 3. Comparison between the present local results and other results available in the literature for the dimensionless temperature profiles close to a single cylinder.

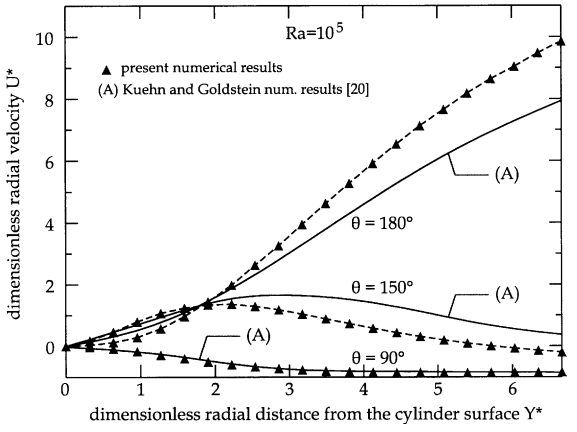

Fig. 4. Comparison between the present local results and other results available in the literature for the dimensionless radial velocity profiles close to a single cylinder.

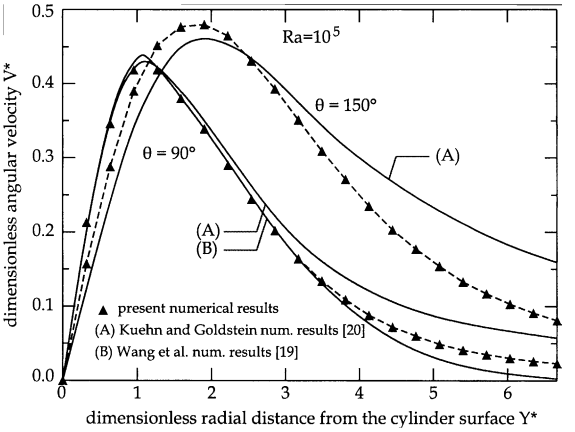

Fig. 5. Comparison between the present local results and other results available in the literature for the dimensionless tangential velocity profiles close to a single cylinder.

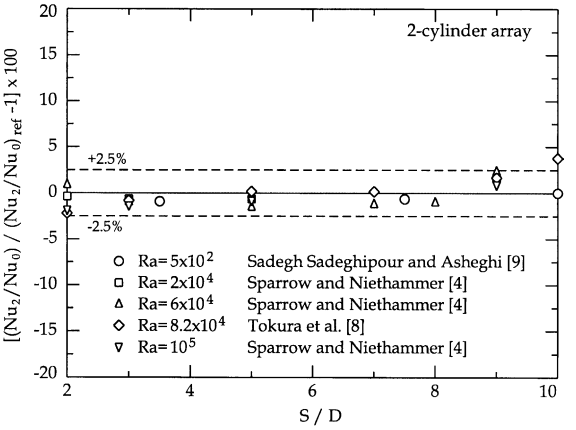

Fig. 6. Comparison between the present results and other experimental results available in the literature for a two-cylinder array.

Finally, the results obtained for a two-cylinder array with tube-spacings in the range between 2 and 10 diameters at several Rayleigh numbers are compared with the experimental data by Sparrow and Niethammer [4], Tokura et al. [8], and Sadegh Sadeghipour and Asheghi [9], showing a meaningfully good agreement, as reported in Fig. 6, where the percent differences of the ratio Nu_2/Nu_0 between the Nusselt number of the upper

cylinder and that of the single cylinder, plotted against the dimensionless tube-spacing S/D, show to lie within the range ±2.5%.

6. Results and discussion

Numerical simulations are performed for $Pr = 0.71$, which corresponds to air, and different values of (a) the Rayleigh number Ra in the range between 5×10^2 and 5×10^5, (b) the number N of cylinders in the range between 1 and 6, and (c) the center-to-center dimensionless separation distance S/D in the range between 2 and a maximum value $(S/D)_{max} = [(H/D)_{max}]/(N - 1)$.

The maximum value of the dimensionless overall height of the tube-array $(H/D)_{max}$ is assumed to be equal to $[(Ra_H)_{cr}/Ra]^{1/3}$, where $(Ra_H)_{cr}$ is the critical value of the Rayleigh number based on the height of the tube-array at which the transition from laminar to turbulent regime occurs. Actually, since data on the transition to the turbulent flow regime for a vertical tube-array are not available in the open literature, a value of the same order of that relevant to the vertical plate, i.e., $\sim 10^9$, is tentatively assumed (whenever this value should be too large, i.e., should the transition occur at a critical value of the Rayleigh number smaller than 10^9, the convergence of the iterative procedure is not achieved).

6.1. Heat transfer from a single cylinder

The results obtained for the single cylinder in the range $10^2 \leqslant Ra \leqslant 10^6$ are presented in Fig. 7, where some of the most prominent correlations for free convection heat transfer from a single cylinder available in the literature, i.e. those by Morgan [22], Raithby and Hollands [23], Kuehn and Goldstein [24], and Churchill and Chu [25], as well as the experimental data by Clemes et al. [26], are also reported for comparison.

An overall good agreement between the present data and those obtained by the previous workers may be noticed. In particular, a rather excellent degree of agreement with the experimental data by Clemes et al. may be observed, which provides further confidence in the numerical code developed.

In contrast, an exception is represented by the Churchill–Chu equation, whose predictions are meaningfully smaller than the present results. Indeed, this was expected, as in the range $10^2 \leqslant Ra \leqslant 10^6$ the Churchill–Chu equation falls well below the data upon which it was based, i.e., the data by Koch [27], Rice [28], and Wamsler [29].

As concerns the other correlations, those proposed by Morgan overpredict slightly the present Nusselt numbers, especially at the largest Rayleigh numbers investigated. This may possibly be explained by considering

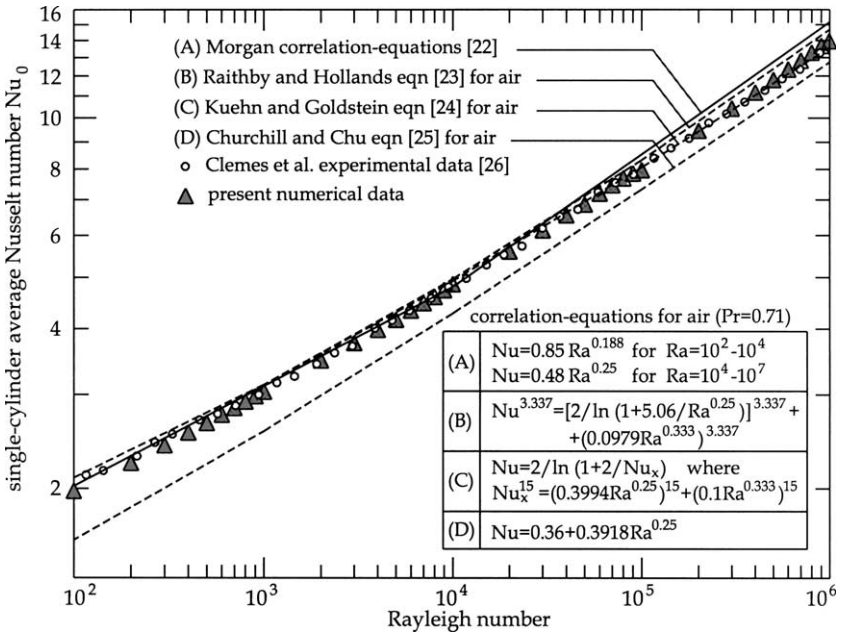

Fig. 7. Comparison between the present results and other results available in the literature for the average Nusselt number of the single cylinder.

that Morgan included also data on liquids, yet, in his correlations he did not consider the effects of the Prandtl number.

The Raithby–Holland and the Kuehn–Goldstein equations are multi-Prandtl number equations based on a conduction layer model, which make use of a Churchill–Usagi blending procedure [30]. However, the different choice of the blending exponent, assumed equal to 3.337 by Raithby and Hollands, and to 15 by Kuehn and Goldstein, brings the Kuehn–Goldstein equation to agree the present data much more closely than the Raithby–Holland equation does.

Finally, all the correlations with slope constant across the entire range of Rayleigh number considered here (typically 0.25, as for, e.g., the correlation-equations proposed by Kutateladze [31] and Fand et al. [32], which are not represented in Fig. 7 for the sake of clarity) seem far too inaccurate, especially at low Rayleigh numbers.

The numerical results obtained for the average Nusselt number of the single cylinder are expressed as a function of the Rayleigh number by the following two distinct simple algebraic relations:

$$Nu = 0.769Ra^{0.198} \quad \text{for } 10^2 \leqslant Ra \leqslant 10^4 \tag{14}$$

with percent standard deviation of error $E_{sd} = 0.41\%$, and range of error E from -0.92% to $+0.71\%$;

$$Nu = 0.537Ra^{0.235} \quad \text{for } 10^4 < Ra \leqslant 10^6 \tag{15}$$

with percent standard deviation of error $E_{sd} = 0.71\%$, and range of error E from -0.99% to $+1.87\%$.

In particular, it seems worth noticing that Eq. (15) is very similar to that proposed by Sparrow and Boessneck, i.e., $Nu = 0.592Ra^{0.23}$, which is based on experiments covering the range of Rayleigh number from 2×10^4 to 2×10^5 [6].

The whole set of the present numerical data may also be correlated through the following binomial algebraic relation of the Churchill–Chu type:

$$Nu = 0.626 + 0.417Ra^{0.25} \quad \text{for } 10^2 \leqslant Ra \leqslant 10^6 \tag{16}$$

with percent standard deviation of error $E_{sd} = 0.89\%$, and range of error E from -1.66% to $+2.03\%$.

It seems interesting to point out that Eq. (16), besides covering the whole range of Rayleigh number considered here with a degree of accuracy of the same order of those of Eqs. (14) and (15), may represent a good option to these equations in all those cases the exponent 0.25 of the Rayleigh number, typical for many laminar-flow situations, should be considered as *inalienable*.

6.2. Heat transfer from individual cylinders in the array

The effects of both the cylinder-spacing S/D and the Rayleigh number Ra on the average heat transfer rate from the ith cylinder in the array are pointed out in Fig. 8, where some representative results are reported for a 4-cylinder array. The ordinate of each diagram is the ratio Nu_i/Nu_0 between the average Nusselt numbers for the ith cylinder and for the single cylinder at same Rayleigh number, so as to highlight in what measure the interactions of the ith cylinder with the upstream and downstream cylinders in the array either enhance or degrade its heat transfer performance relative to that of a single cylinder. It may be seen that at any Rayleigh number, for any tube-array, the heat transfer rate at the bottom cylinder is substantially identical to that for a single cylinder, even for the closest separation distance investigated. In contrast, the degree of enhancement or degradation of the heat transfer rate at any downstream cylinder is strongly dependent on the cylinder-spacing, whilst showing only a slight dependence on the Rayleigh number. In more details, at any Rayleigh number investigated, for the smaller cylinder-spacings, degradation is generally the rule, whilst, at the larger separation distances, enhancement predominates, as found also in the aforementioned previous studies carried out on this same subject.

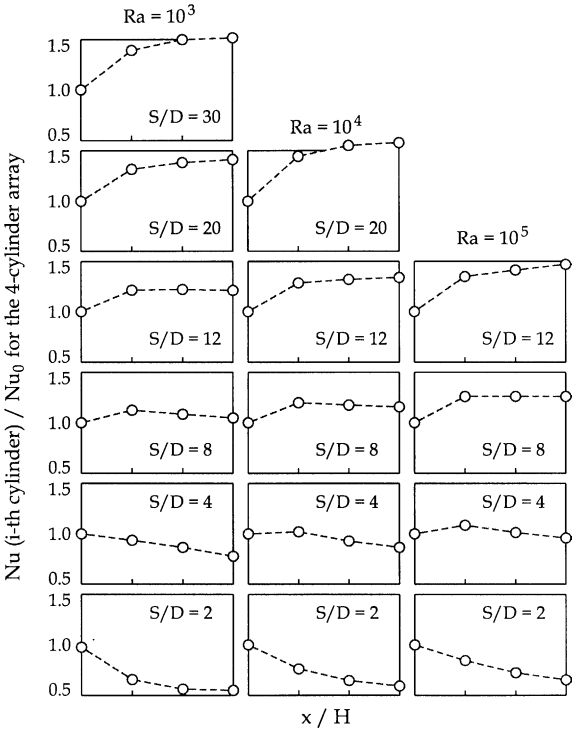

Fig. 8. Distributions of the ratio Nu_i/Nu_0 vs. x/H for a four-cylinder array, at different values of Ra and S/D.

It seems worth noticing that for tube-arrays consisting of the same number of cylinders, the same distribution of the ratio Nu_i/Nu_0 vs. x/H may be obtained at different Rayleigh numbers, provided that the cylinder-spacing S/D is decreased as the Rayleigh number Ra is

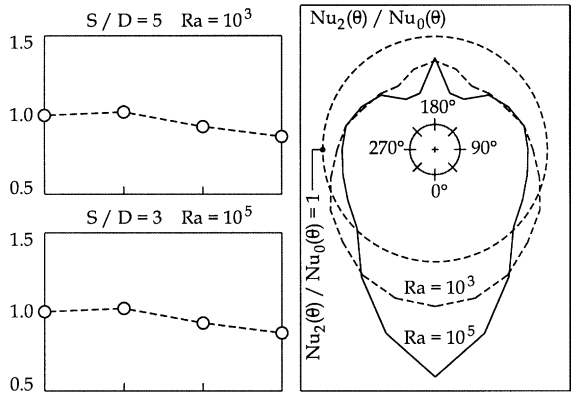

Fig. 9. Polar distributions of the ratio $Nu_2(\theta)/Nu_0(\theta)$ for the second cylinder in a four-cylinder array, at $Ra = 10^3$ and $S/D = 5$, and at $Ra = 10^5$ and $S/D = 3$.

increased. This is, e.g., the case of the 4-cylinder array at $Ra = 10^3$ with $S/D = 5$, and at $Ra = 10^5$ with $S/D = 3$, as reported in the left panels of Fig. 9. However, leaving aside the bottom cylinder (whose behavior, as said, is the same as for the single cylinder), the local heat transfer performance of any ith downstream cylinder relative to that of a single cylinder, i.e., the local value of the ratio $Nu_i(\theta)/Nu_0(\theta)$, depends on the Rayleigh number considered. This is shown in the right panel of Fig. 9, where the polar distributions of the ratio $Nu_2(\theta)/Nu_0(\theta)$ between the local Nusselt numbers for, e.g., the second cylinder and the single cylinder at the same angle θ, are depicted for the two cases indicated above.

As concerns the effects of the number of cylinders N upon the heat transfer rate at the ith cylinder, the distributions of the ratio Nu_i/Nu_0 along tube-arrays consisting of two to six cylinders with spacings $S/D = 2$, 3, and 4, are reported in Fig. 10 for $Ra = 10^4$. It may be noticed

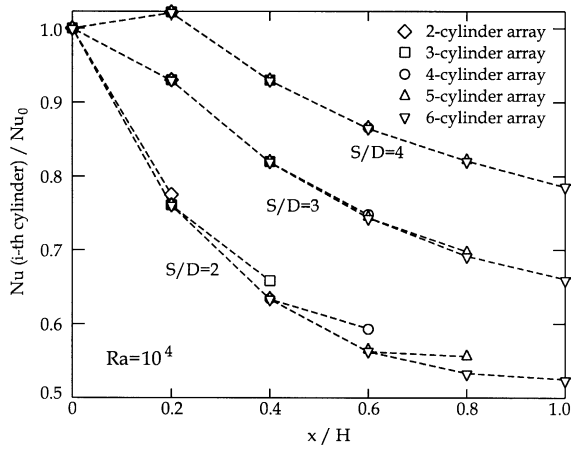

Fig. 10. Distributions of the ratio Nu_i/Nu_0 through tube-arrays of two to six cylinders, at $Ra = 10^4$ and for different values of S/D.

that for $S/D > 2$ the average heat transfer rate at the ith cylinder is practically independent of the number of downstream cylinders. This means that the heat transfer rate at the ith cylinder is determined only by the interference with the upstream cylinders, thus implying that the problem may be addressed to as a *one-way coordinate* problem. However, for $S/D = 2$ a slight increase in the heat transfer rate at the ith cylinder may be observed in all those cases the ith cylinder is the top cylinder of the array, i.e., whenever $i = N$. This may be explained by considering that, for $i < N$ at close spacing, the buoyant flow around the ith cylinder cannot penetrate completely the space between the consecutive ith and $(i + 1)$th cylinders, which implies that the region of the rear stagnation point of the ith cylinder is wider than the corresponding region for the top cylinder of the array, and then that a smaller amount of heat is exchanged at its upper surface.

The whole set of numerical results obtained for the average Nusselt number Nu_i of any individual ith cylinder in the array may be correlated to the Rayleigh number Ra, to the cylinder location relative to the center of the bottom cylinder x/H, and to the ordinal number N_i of the cylinder, by the following two distinct transcendent equations, as also shown in Fig. 11:

$$\begin{aligned} Nu_{i\mathrm{th}} &= Ra^{0.25}\{0.364\ln[(x/D)^{0.4}/N_i^{0.9}] + 0.508\} \\ &2 \leqslant N_i \leqslant 6 \quad 2(N_i - 1) < x/D \leqslant 8 + N_i \\ &5 \times 10^2 \leqslant Ra \leqslant 5 \times 10^5 \end{aligned} \tag{17}$$

with percent standard deviation of error $E_{\mathrm{sd}} = 3.19\%$, and range of error E from -5.07% to $+7.97\%$;

$$\begin{aligned} Nu_{i\mathrm{th}} &= Ra^{0.25}\{0.587\ln[(x/D)^{0.33}/N_i^{0.5}] + 0.350\} \\ &2 \leqslant N_i \leqslant 6 \quad 8 + N_i < x/D \leqslant (10^9/Ra)^{0.333} \\ &5 \times 10^2 \leqslant Ra \leqslant 5 \times 10^5 \end{aligned} \tag{18}$$

with percent standard deviation of error $E_{\mathrm{sd}} = 3.27\%$, and range of error E from -5.93% to $+7.96\%$.

Finally, from the analysis of Figs. 8 and 11, it is evident that in the present study the maximum for the heat transfer rate, which was found experimentally by some of the previous workers at different optimal tube-spacings, has not been detected, at least within the limits of the largest separation distances considered here. Taking into account the aforementioned shallowness of such maximum, as well as the reported discrepancies in the values of the optimal tube-spacing (from 8 to 120 diameters), this may possibly be ascribed to the natural disturbances which inevitably arise in the course of the experiments, whose contribution cannot be accounted for in a numerical simulation model. In fact, these natural disturbances, which are function of several factors, as, e.g., the isolation of the test room, the nearess of free surfaces, and the quiescence of the ambient surroundings, to name a few, may decrease the stability of the

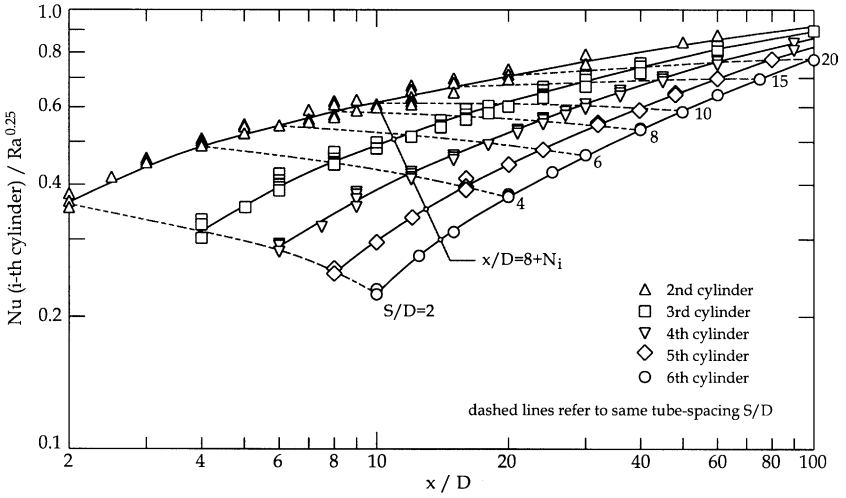

Fig. 11. Distributions of the ratio $Nu_i/Ra^{0.25}$ vs. x/H for the downstream cylinders.

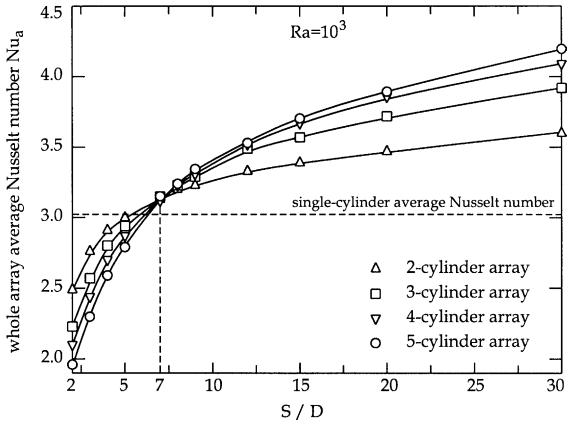

Fig. 12. Distributions of Nu_a vs. S/D for tube-arrays consisting of different numbers of cylinders, at $Ra = 10^3$.

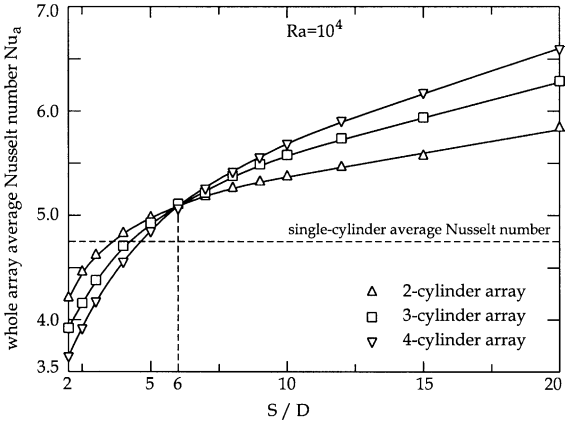

Fig. 13. Distributions of Nu_a vs. S/D for tube-arrays consisting of different numbers of cylinders, at $Ra = 10^4$.

warm plume spawned by the upstream cylinder. This means that, from a "critical" distance onwards, the rising plume may start swaying increasingly with height up to breaking, which would clearly affect the heat transfer rate at the downstream cylinder, whose thermal behavior would ultimately degrade.

6.3. Heat transfer from the whole tube-array

The distributions of the average Nusselt number of the whole array Nu_a versus the tube-spacing S/D for different numbers of cylinders in the array, are reported in Figs. 12–14, for Rayleigh numbers 10^3, 10^4, and 10^5, respectively.

As expected, the average Nusselt number of the whole tube-array increases with increasing the Rayleigh number. In addition, Nu_a increases also with S/D,

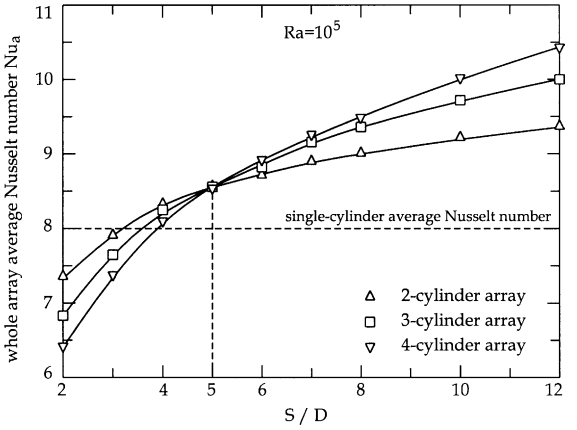

Fig. 14. Distributions of Nu_a vs. S/D for tube-arrays consisting of different numbers of cylinders, at $Ra = 10^5$.

according to a decreasing slope. As far as the effects of the number of cylinders is concerned, it may be seen that the overall heat transfer rate may either increase or decrease with increasing the number of cylinders in the array, according as the cylinder-spacing is larger or smaller than a specific value S^*/D, which is found to decrease with increasing the Rayleigh number. In particular, all the values obtained for S^*/D may be pretty well correlated to the Rayleigh number through the following linear equation:

$$S^*/D = 10 - \log(Ra) \tag{19}$$

with percent standard deviation of error $E_{sd} = 0.28\%$ and range of error E from -0.54% to $+0.65\%$.

Of course, once the tube-spacing is set equal to S^*/D, the average Nusselt number of the whole array is independent of the number of cylinders in the array. This means that, for the downstream cylinders, the opposite effects which originate from the upward-moving air flow compensate each other, i.e., the enhancing effect of the higher air velocity counterbalances the degrading effect of the larger air temperature.

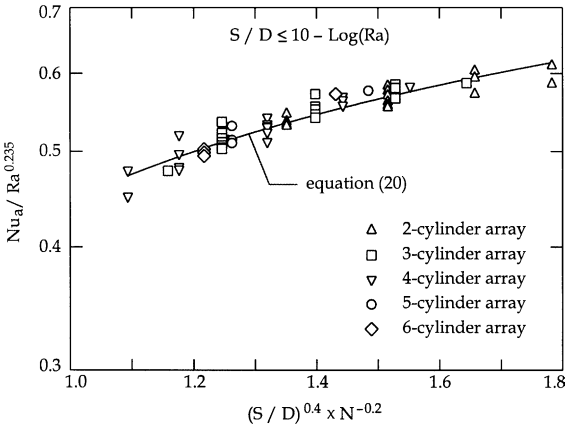

Fig. 15. Comparison between Eq. (20) and the numerical results.

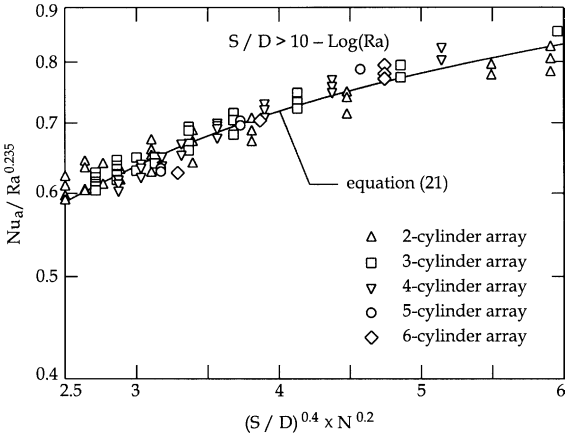

Fig. 16. Comparison between Eq. (21) and the numerical results.

The numerical results obtained for the average Nusselt number of the whole tube-array Nu_a may be correlated to the Rayleigh number Ra, to the cylinder-spacing S/D, and to the number N of cylinders in the array, by the following two distinct transcendent equations, as also shown in Figs. 15 and 16:

$$Nu_a = Ra^{0.235}\{0.292\ln[(S/D)^{0.4} \times N^{-0.2}] + 0.447\}$$
$$2 \leqslant N \leqslant 6 \quad 5 \times 10^2 \leqslant Ra \leqslant 5 \times 10^5 \tag{20}$$
$$S/D \leqslant 10 - \log(Ra)$$

with percent standard deviation of error $E_{sd} = 2.25\%$, and range of error E from -4.79% to $+5.27\%$;

$$Nu_a = Ra^{0.235}\{0.277\ln[(S/D)^{0.4} \times N^{0.2}] + 0.335\}$$
$$2 \leqslant N \leqslant 6 \quad 5 \times 10^2 \leqslant Ra \leqslant 5 \times 10^5 \tag{21}$$
$$S/D > 10 - \log(Ra)$$

with percent standard deviation of error $E_{sd} = 2.72\%$, and range of error E from -6.40% to $+6.09\%$.

7. Conclusions

Steady laminar free convection from flat vertical arrays of horizontal isothermal cylinders set in free air has been studied numerically through a specifically developed computer-code based on the SIMPLE-C algorithm. Simulations have been performed for arrays of 2–6 circular cylinders, for center-to-center separation distances from 2 up to more than 50 cylinder-diameters, and for values of the Rayleigh number based on the cylinder-diameter in the range between 5×10^2 and 5×10^5. Heat transfer dimensionless correlating equations with rather acceptable standard deviations and absolute values of the maximum relative error, have been developed for any individual cylinder in the array and for the whole tube-array. New correlation-equations for the calculation of the heat transfer rate from a single cylinder to the surrounding air have also been proposed and compared to the most prominent correlations available in the open literature.

The main results obtained in the present study may be summarized as follows:

(a) At any Rayleigh number, and for any tube-array, the heat transfer rate at the bottom cylinder is substantially identical to that for a single cylinder, even for the closest center-to-center separation distance investigated, i.e. $S/D = 2$.

(b) The heat transfer rate at any downstream cylinder may either enhance or degrade with respect to that for a single cylinder, depending on the location of the cylinder in the array and on the tube-spacing. In particular, at any Rayleigh number investigated, degradation is generally the rule at the smaller tube-spacings, whilst enhancement predominates at the larger ones.

(c) For arrays consisting of the same number of cylinders, the same distribution of the ratio Nu_i/Nu_0 vs. x/H may well be obtained at different Rayleigh numbers, provided that the cylinder-spacing S/D is decreased as the Rayleigh number Ra is increased.

(d) For tube-spacings larger than the closest investigated, i.e. for $S/D > 2$, the heat transfer rate at the ith cylinder of the array is practically independent of the number of downstream cylinders. This means that the heat transfer rate at the ith cylinder is determined only by the interference with the upstream cylinders, thus implying that the problem may be addressed to as a one-way coordinate problem.

(e) The amount of heat exchanged by the whole array increases with the tube-spacing, according to a decreasing slope. In addition, the overall heat transfer rate from the array to the surrounding air may either increase or decrease with increasing the number of cylinders in the array, according as the tube-spacing is larger or smaller than a specific value which reduces slightly with increasing the Rayleigh number.

References

[1] E.R.G. Eckert, E.E. Soehngen, Studies on heat transfer in laminar free convection with the Zehnder-Mach interferometer, AF Technical Report, 5747, USAF Air Material Command, Wright-Paterson Air Force Base, Ohio, 1948.

[2] J. Lieberman, B. Gebhart, Interaction in natural convection from an array of heated elements, experimental, Int. J. Heat Mass Transfer 12 (1969) 1385–1396.

[3] G.F. Marsters, Arrays of heated horizontal cylinders in natural convection, Int. J. Heat Mass Transfer 15 (1972) 921–933.

[4] E.M. Sparrow, J.E. Niethammer, Effect of vertical separation distance and cylinder-to-cylinder temperature imbalance on natural convection for a pair of horizontal cylinders, J. Heat Transfer 103 (1981) 638–644.

[5] B. Gebhart, L. Pera, A.W. Schorr, Steady laminar natural convection plumes above a horizontal line heat source, Int. J. Heat Mass Transfer 13 (1970) 161–171.

[6] E.M. Sparrow, D.S. Boessneck, Effect of traverse misalignment on natural convection from a pair of parallel, vertically stacked, horizontal cylinders, J. Heat Transfer 105 (1983) 241–247.

[7] R.G. Hunter, J.C. Chato, Natural-convection heat transfer from parallel, horizontal cylinders, ASHRAE 93 (1987) 767.

[8] I. Tokura, H. Saito, K. Kisinami, K. Muramoto, An experimental study of free convection heat transfer from a horizontal cylinder in a vertical array set in free space between parallel walls, J. Heat Transfer 105 (1983) 102–107.

[9] M. Sadegh Sadeghipour, M. Asheghi, Free convection heat transfer from arrays of vertically separated horizontal cylinders at low Rayleigh numbers, Int. J. Heat Mass Transfer 37 (1994) 103–109.

[10] B. Farouk, S.I. Guceri, Natural convection from horizontal cylinders in interacting flow fields, Int. J. Heat Mass Transfer 26 (1983) 231–243.

[11] R. Chouikh, A. Guizani, M. Maalej, A. Belghith, Numerical study of the laminar natural convection flow around an array of two horizontal isothermal cylinders, Int. Comm. Heat Mass Transfer 26 (1999) 329–338.

[12] B.E. Launder, T.H. Massey, The numerical prediction of viscous flow and heat transfer in tube banks, J. Heat Transfer 100 (1978) 565–571.

[13] J.P. Van Doormaal, G.D. Raithby, Enhancements of the simple method for predicting incompressible fluid flows, Numer. Heat Transfer 11 (1984) 147–163.

[14] S.V. Patankar, D.B. Spalding, A calculation procedure for heat, mass and momentum transfer in three-dimensional parabolic flows, Int. J. Heat Mass Transfer 15 (1972) 1787–1797.

[15] B.P. Leonard, A stable and accurate convective modelling procedure based on quadratic upstream interpolation, Comput. Methods Appl. Mech. Eng. 19 (1979) 59–78.

[16] S.V. Patankar, Numerical Heat Transfer and Fluid Flow, Hemisphere Publ. Co., Washington, DC, 1980.

[17] S.V. Patankar, Recent developments in computational heat transfer, J. Heat Transfer 110 (1988) 1037–1045.

[18] T. Saitoh, T. Sajiki, K. Maruhara, Bench mark solutions to natural convection heat transfer problem around a horizontal circular cylinder, Int. J. Heat Mass Transfer 36 (1993) 1251–1259.

[19] P. Wang, R. Kahawita, T.H. Nguyen, Numerical computation of the natural convection flow about a horizontal cylinder using splines, Numer. Heat Transfer 17 (1990) 191–215.

[20] T.H. Kuehn, R.J. Goldstein, Numerical solution to the Navier–Stokes equations for laminar natural convection about a horizontal isothermal circular cylinder, Int. J. Heat Mass Transfer 23 (1980) 971–979.

[21] T. Chiang, J. Kaye, On laminar free convection from a horizontal cylinder, in: Proceedings of the Fourth National Congress of Applied Mechanics, 1962, pp. 1213–1219.

[22] V.T. Morgan, The overall convective heat transfer from smooth circular cylinders, Adv. Heat Transfer 11 (1975) 199–264.

[23] G.D. Raithby, K.G.T. Hollands, Laminar and turbulent free convection from elliptic cylinders with a vertical plate and horizontal circular cylinder as special cases, J. Heat Transfer 98 (1976) 72–80.

[24] T.H. Kuehn, R.J. Goldstein, Correlating equations for natural convection heat transfer between horizontal circular cylinders, Int. J. Heat Mass Transfer 19 (1976) 1127–1134.
[25] S.W. Churchill, H.H.S. Chu, Correlating equations for laminar and turbulent free convection from a horizontal cylinder, Int. J. Heat Mass Transfer 18 (1975) 1049–1053.
[26] S.B. Clemes, K.G.T. Hollands, A.P. Brunger, Natural convection heat transfer from long horizontal isothermal cylinders, J. Heat Transfer 116 (1994) 96–104.
[27] W. Koch, Geshundh.-Ing. 22 (1927) 1–27.
[28] C.W. Rice, Free and forced convection of heat from bodies of simple shape in gases and liquids, International Critical Tables, vol. 5, McGraw-Hill, New York, 1929, pp. 234–236.
[29] F. Wamsler, Die wärmeabgabe geheizter körper an luft, Mitt. Forsch. Hefte 98/99 (1911) 1–45.
[30] S.W. Churchill, R. Usagi, A general expression for the correlation of rates of transfer and other phenomena, AIChE J. 18 (1972) 1121–1128.
[31] S.S. Kutateladze, Fundamentals of Heat Transfer, Academic Press, New York, 1963, pp. 288–297.
[32] R.M. Fand, E.W. Morris, M. Lum, Natural convection heat transfer from horizontal cylinders to air, water and silicone oils for Rayleigh numbers between 3×10^2 and 2×10^7, Int. J. Heat Mass Transfer 20 (1977) 1173–1184.